

Cite this: *Green Chem.*, 2014, **16**, 2204  
 2204

## Direct conversion of chitin into a N-containing furan derivative†

Xi Chen,<sup>a</sup> Shu Ling Chew,<sup>a</sup> Francesca M. Kerton<sup>b</sup> and Ning Yan\*<sup>a</sup>

This paper describes the direct conversion of chitin into a nitrogen-containing (N-containing) furan derivative (3A5AF) for the first time. Under optimized conditions, the yield of 3A5AF reaches 7.5% with ca. 50% chitin conversion by using boric acid and alkaline chlorides as additives, and NMP as a solvent. A variety of other compounds, including levoglucosanone, 4-(acetylamino)-1,3-benzenediol, acetic acid and chitin-humins, have been identified as side products, based on which a plausible reaction network involved in the process is proposed. Mechanistic investigation by NMR studies and poison tests confirms the formation of a boron complex intermediate during the reaction, shedding light on the promotional effects of boric acid. Kinetic studies show that the depolymerization of the chitin crystalline region is rate-determining, and therefore disruption of the hydrogen bonding in the crystalline region of chitin, either before or during the reaction, is the key to further improving the reaction yields.

Received 28th November 2013,  
 Accepted 4th January 2014

DOI: 10.1039/c3gc42436g  
[www.rsc.org/greenchem](http://www.rsc.org/greenchem)

## 1. Introduction

The imperative to reduce society's dependence on crude oil has led to significant research efforts at the conversion of biomass.<sup>1,2</sup> So far, remarkable progress has been made in the conversion of lignocellulosic biomass into bioethanol<sup>3,4</sup> and value-added platform chemicals.<sup>5–14</sup> On the other hand, much less attention has been directed to the utilization of chitin,<sup>15</sup> which is a major component of the exoskeletons of insects and crustaceans<sup>16</sup> and the second most abundant biopolymer on earth. The chemical structure of chitin is highly similar to cellulose, consisting of *N*-acetyl-*D*-glucosamine (NAG) monosaccharide units as the building blocks linked together by  $\beta$ -glycosidic bonds (see Fig. 1). Chitin has an underestimated but remarkable potential for the production of renewable, value-added chemicals, especially N-containing compounds, as it comprises 7 wt% of biologically-fixed nitrogen. Nowadays, the manufacture of N-containing chemicals is typically laborious and energy intensive starting from high temperature, high pressure ammonia synthesis. Chitin is an attractive, sustainable and cheap organic nitrogen resource that holds the potential to revolutionize the production of certain chemicals bearing nitrogen.

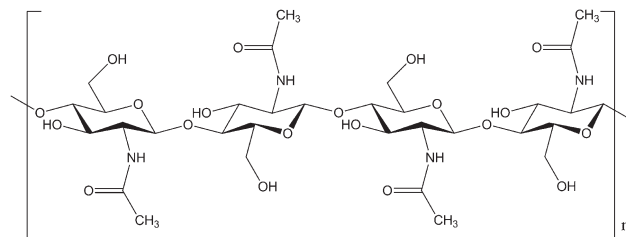


Fig. 1 The chain structure of chitin polymer.

Current utilization of chitin remains very limited. Chemical derivatizations have been frequently conducted to modify the properties of chitin.<sup>17–19</sup> However, these are based on stoichiometric chemical reactions on the substitution groups on chitin polymer chains, and therefore are unable to produce non-polymeric chemicals. Pyrolysis or radiolysis of chitin/chitosan to produce volatile aromatic heterocyclic compounds such as pyrazines, pyridines, pyrroles and furans has been reported.<sup>20–22</sup> Nevertheless, these methods cannot achieve a selective degradation resulting in trace amounts of products. Hydrolysis of chitin by enzymes or concentrated acids affords NAG and oligomers, but this route suffers from low efficiency, environmental issues and limited product diversity.<sup>23,24</sup> Starting from chitin, the production of 5-(chloromethyl)furfural,<sup>25</sup> levulinic acid (LA),<sup>26</sup> and 5-hydroxymethylfurfural (5-HMF)<sup>27</sup> with yields ranging from 9 to 11% was reported very recently. Unfortunately, the precious, biologically fixed nitrogen was lost during the transformation. To the best of our knowledge, direct conversion of chitin into value-added nitrogen-containing chemicals with noticeable yields has not yet been realized.

<sup>a</sup>Department of Chemical and Biomolecular Engineering, National University of Singapore, 4 Engineering Drive 4, 117576, Singapore. E-mail: ning.yan@nus.edu.sg

<sup>b</sup>Department of Chemistry, Memorial University of Newfoundland, St. John's, NL A1B 3X7, Canada

† Electronic supplementary information (ESI) available: Details of solvent/additive screening and optimization, EA/GPC characterization and additional mechanistic investigation. See DOI: 10.1039/c3gc42436g



In 2012, the transformation of NAG into 3-acetamido-5-acetyl furan (3A5AF) was reported by dehydration reactions, demonstrating the feasibility of obtaining N-containing furan derivatives from chitin monomers.<sup>28,29</sup> Encouraged by this advancement, we for the first time tested the possibility of producing 3A5AF directly from chitin, which, in principle, could be obtained by combining chitin hydrolysis and NAG dehydration. In this paper, 6 solvents, 26 additives and their combinations were evaluated. For the optimized system, detailed studies concerning the reaction kinetics, reaction pathway, effects of water as an additive, and mechanistic investigation using NMR and poison tests were conducted.

## 2. Experimental

### 2.1. Materials

Chitin was purchased from Wako Pure Chemical Industry. Boric acid was purchased from Amresco. Sodium chloride (NaCl) was purchased from Schedelco. Lithium chloride (LiCl) and dimethylacetamide (DMA) were purchased from Alfa Aesar. *N*-Acetyl-D-glucosamine (NAG), iron(II), tin(II), barium and cesium chloride salts (FeCl<sub>2</sub>, SnCl<sub>2</sub>, BaCl<sub>2</sub> and CsCl, respectively), *N*-methyl-2-pyrrolidone (NMP) and dimethyl sulfoxide (DMSO) were purchased from Sigma Aldrich. Dimethylformamide (DMF) and glycerine (Gly) were from Fisher Scientific. Ethylene glycol (EG) was purchased from Fluka. DMSO-d<sub>6</sub> was purchased from VWR Singapore. Other chemicals, such as copper chloride (CuCl<sub>2</sub>), tungsten oxide (WO<sub>3</sub>), cobalt chloride (CoCl<sub>2</sub>), nickel chloride (NiCl<sub>2</sub>) and calcium chloride (CaCl<sub>2</sub>), were obtained from Sinopharm Chemical Reagent (SCR). All chemicals were used as received.

### 2.2. General procedure

Under optimized conditions, chitin (100 mg, 0.5 mmol based on the NAG monomer) was placed in a thick-wall glass tube (35 mL). Following that a magnetic stir bar, boric acid (122 mg, 2.0 mmol), NaCl (58 mg, 1.0 mmol) and anhydrous NMP (3 mL) were added. The tube was sealed by a Teflon stopper and placed into a pre-heated oil bath at 215 °C for 1 h under a stirring speed of 400 rpm. After the reaction, the reaction mixture was cooled down to room temperature. Methanol (15 mL) was added. After thorough mixing, a portion of the liquid sample (1 mL) was filtered by a PTFE syringe filter with a 0.2 µm pore size before analyzing by high-performance liquid chromatography (HPLC).

It is noteworthy that all the reactions were carried out in a similar manner whilst varying the following parameters: additive (or additive amount), solvent, reaction time and temperature.

HPLC analysis was performed on an Agilent 1200 Series (Agilent Technologies, Germany) LC system by using an Agilent ZORBAX Eclipse carbon-18 column. The mobile phase was 83% water and 17% acetonitrile. The flow rate was kept at 0.5 mL min<sup>-1</sup> with a run-time of 20 min. A UV-vis detector

setting at 230 nm was used to analyze the product. 3A5AF standard was prepared following a literature method<sup>28</sup> and the purity verified by nuclear magnetic resonance (NMR) spectroscopy. A calibration curve (Fig. S1†) was generated with a series of 3A5AF standard solutions and used for quantification of the product.

To obtain the conversion of chitin, the reaction mixture was centrifuged after the reaction. The remaining solid was washed with water three times and dried in an oven over 24 h at 70 °C and weighed. The conversion of chitin is calculated as:

$$\text{Conversion} = \frac{\text{Starting chitin (mg)} - \text{Residual solid (mg)}}{\text{Starting chitin (mg)}} \times 100\%$$

### 2.3. Identification of other products

After the reactions, the liquid samples from six parallel experiments were combined. Then, reduced pressure distillation was applied for the removal of NMP solvent. The Edwards Rotary Vane Pump (Model RV3) with an ultimate pressure of 0.002 mbar was used. The liquids were put into a round bottle flask and heated at about 90 °C under vacuum. After the majority of the solvent was removed, column chromatography was employed for separation using silica gel with particle size ranging from 40 to 63 µm as the stationary phase and 5% methanol and 95% dichloromethane as the mobile phase. Afterwards the collected fractions were concentrated by a rotary evaporator and analyzed by gas chromatography-mass spectrometry (GC-MS).

### 2.4. Characterization

X-ray powder diffraction (XRD) was performed on a Bruker D8 Advanced Diffractometer with Cu K $\alpha$  radiation at 40 kV. Gel permeation chromatography (GPC) analysis was carried out with a system equipped with a Waters 2410 refractive index detector, a Waters 515 HPLC pump and two Waters styragel columns (HT 3 and HT 4) using DMF as an eluent at a flow rate of 1 mL min<sup>-1</sup> at 25 °C. The raw data were processed using narrow polydispersity polystyrene standards and calibration using the software Breeze. Fourier transform infrared spectroscopy (FTIR) was conducted on a Bio-Rad FTS-3500 ARX instrument. GC-MS was performed on an Agilent 7890A GC system with 7693 Autosampler and 5975C inert MSD with triple-axis detector. Elemental analysis (EA) was conducted using an Elementar Vario Micro Cube and the degree of acetylation (DA) was calculated according to EA analysis.<sup>30</sup> Proton, boron and carbon NMR (<sup>1</sup>H, <sup>11</sup>B and <sup>13</sup>C NMR) were performed on a Bruker ultrashield 400 plus spectrometer.

$$\text{DA} = [(C/N - 5.14)/1.72] \times 100\%$$

where C/N is the ratio (w/w) of carbon to nitrogen.



### 3. Results and discussion

#### 3.1. Solvent screening

Similar to cellulose,<sup>31–33</sup> one of the major challenges for chitin conversion is its robust crystal structure with extensive inter- and intra-hydrogen bonds among the polymer chains.<sup>34,35</sup> Solvent or solvent systems that are able to dissolve chitin should prove advantageous in its transformation. Previously, dipolar aprotic solvents combined with metal salts, such as 5–7% LiCl/NMP and LiCl/DMA systems, have been reported to dissolve chitin.<sup>36</sup> We started by screening 6 solvents including DMA, DMF, DMSO, NMP, EG and Gly. The first four solvents are commonly used for sugar dehydration<sup>37–41</sup> whereas EG and Gly are selected because their hydroxyl groups may disrupt the hydrogen bonding network in chitin. When chitin was dispersed in these 6 solvents at 195 or 225 °C for 1 h, no 3A5AF was detected. LiCl (5 wt%, based on solvent) was added into these solvents as a solubility enhancing agent, but the yield of 3A5AF remained at 0% in all cases. These two series of experiments indicate that chitin dehydration to 3A5AF could not be obtained by thermal decomposition under the temperatures investigated, irrespective of the solvent used.

To differentiate the solvent effect in converting chitin into 3A5AF, different additives that are active in sugar dehydration, such as HCl,<sup>42–44</sup> boric acid,<sup>45–47</sup> and their combination with LiCl, were employed. The results are shown in Fig. S2.† By adding HCl, 3A5AF was obtained in DMA, DMF and NMP (2.3, 1.1 and 3.0% respectively). By adding boric acid, 3A5AF was obtained in DMA, DMF, DMSO and NMP. No 3A5AF was detected in EG and Gly under these conditions. The best performance was achieved in the presence of boric acid and LiCl in NMP, reaching a 3A5AF yield of 5%. From the above DMA, DMF, DMSO and NMP are all suitable solvents for chitin conversion but NMP appears to be the most effective. Previously, DMF and DMA were identified to be the best solvents for chitin monomer dehydration, and NMP was slightly less effective. The different performances may be ascribed to the structure difference of chitin and NAG. DMA and DMF are smaller in their molecular size, which may favor the solute–solvent interaction in sugar monomer conversion. On the other hand, a major challenge in chitin conversion is its low solubility, and therefore NMP is more effective considering that LiCl/NMP represents a classic solvent system for chitin dissolution. After that, the system was further optimized by conducting the reaction at different temperatures and with a different solvent to chitin ratio (Fig. S3 & S4†). The optimal temperature was identified to be 215 °C and the optimal solvent to chitin ratio to be 3 mL to 100 mg.

#### 3.2. Additive screening

We systematically evaluated the performance of a wide range of additives for chitin conversion to 3A5AF in NMP under selected conditions. These additives included 13 metal chlorides, 6 organic/simple inorganic acids, 5 bases and 3 heteropolyacids (see Fig. 2a). Heteropolyacids, which have been

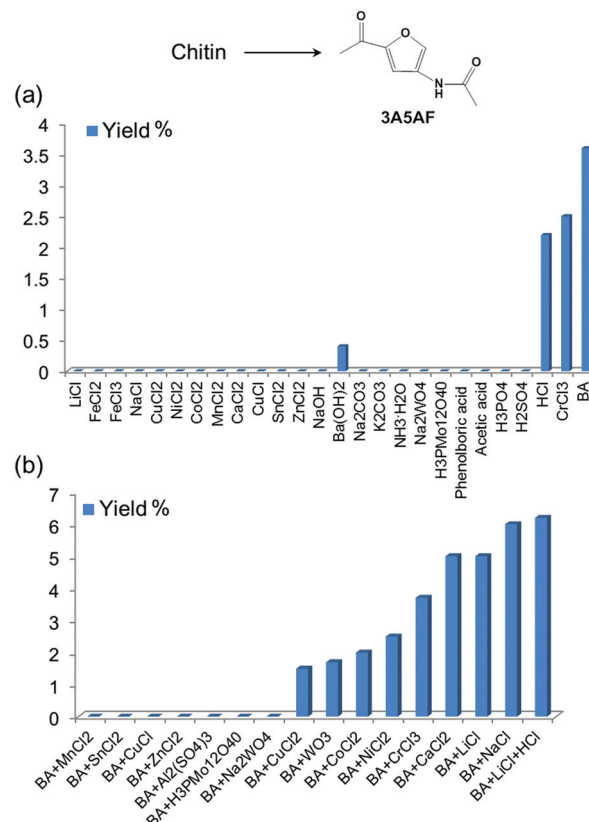


Fig. 2 Additive screening for chitin conversion into 3A5AF. Reaction conditions: 215 °C, 1 h, NMP (3 mL), chitin (100 mg), 200 mol% additive based on chitin monomer (400 mol% for boric acid). (a) Single component screening; (b) combinations of additives (BA is short for boric acid).

reported to be excellent catalysts for glucose/cellulose dehydration,<sup>48–50</sup> did not produce any 3A5AF. Bases were not effective either. Ba(OH)<sub>2</sub> is the only basic additive that produced 3A5AF, but the yield was very low (0.4%). Metal chlorides are widely used as catalysts for glucose dehydration to 5-HMF,<sup>51–55</sup> and in our experiments CrCl<sub>3</sub> effectively promoted 3A5AF formation (2.5%). Organic acids such as phenylboronic acid and acetic acid are not able to facilitate the reaction. Among the inorganic acids, HCl is the only one effective for chitin conversion to 3A5AF with a yield of 2.2%, indicating the promotional effect of chloride ion in the reaction. This is consistent with a previous finding in NAG, glucose and cellulose conversion where chloride played an important role.<sup>28,45,56,57</sup> It is very likely that chloride acts as a promoter to disrupt the hydrogen bonding in the substrate rather than as a catalyst, considering that the majority of metal chlorides are inactive in 3A5AF formation. Boric acid is the most effective additive for the reaction with a 3A5AF yield of 3.6%. Presumably, boric acid facilitates both the hydrolysis of chitin and the dehydration due to its acidity and this gives rise to its promotional ability. In previous studies it was proposed that boric acid coordinated with the hydroxyl groups of glucose and this enables its dehydration to generate 5-HMF.<sup>47</sup>

In an attempt to obtain higher yields, combinations of additives were investigated. Since boric acid is the most effective single component additive, the combinations are based on boric acid and another additive (see Fig. 2b). Interestingly, the combination of boric acid with some metal chlorides, such as  $MnCl_2$ ,  $SnCl_4$ ,  $CuCl$  and  $ZnCl_2$ , and heteropolyacids did not afford any 3A5AF from chitin. Boric acid with  $CuCl_2$ ,  $WO_3$ ,  $CoCl_2$  and  $NiCl_2$  led to 3A5AF formation but the yield was lower than when using boric acid alone. On the other hand, the combinational use of boric acid with  $CrCl_3$ ,  $LiCl$ ,  $NaCl$  and  $CaCl_2$  resulted in enhanced yields. Since the highest yields were obtained by using the combination of boric acid and alkali/alkaline earth metal chlorides, more detailed optimizations were conducted on a series of alkali/alkaline earth metal chlorides, or HCl, combined with boric acid. Different amounts of additives were investigated and the results are compiled in Fig. S5.† This led to the discovery of a few systems that are able to produce *ca.* 6% 3A5AF directly from chitin within one hour. These include: (1) the combination of 400 mol% boric acid and 200 mol%  $NaCl$ ; (2) the combination of 200 mol% boric acid and 100 mol%  $LiCl$ ; (3) the tri-component combination of 400 mol% boric acid, 200 mol%  $LiCl$  and 100 mol% HCl. The last combination is slightly better than the other two, reaching a 3A5AF yield of 6.2%. The addition of HCl is assumed to facilitate the hydrolysis of chitin.

### 3.3. Reaction kinetics

The combination of boric acid and  $NaCl$  was chosen to study the chitin conversion and the 3A5AF yield as a function of reaction time (see Fig. 3). Note that if the chitin conversion is calculated based on the recovered solids after reaction, the value will be underestimated if insoluble char or humins forms during the reaction. In the first few minutes, the product was not yet formed despite a chitin conversion of 15.5%. Normally, chitin has an amorphous and a crystalline part,<sup>16,58</sup> and amorphous chitin is more easily converted. The crystalline index for chitin ranges from 70 to 80%. Therefore the initial conversion may be ascribed to the conversion of amorphous chitin, which depolymerized and generated soluble, low-molecular weight oligomers. As the reaction proceeded from 5 min to 2 hours, the chitin conversion and 3A5AF yield increase simultaneously. It is not unreasonable to

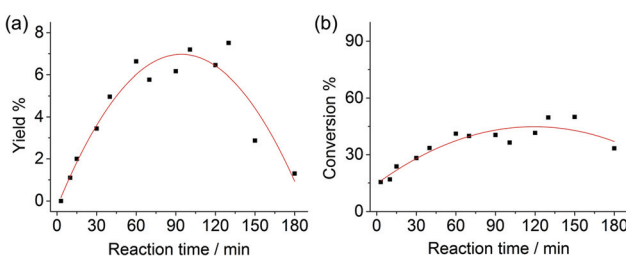


Fig. 3 (a) 3A5AF yield as a function reaction time; (b) chitin conversion as a function reaction time. Reaction conditions: 215 °C, NMP (3 mL), chitin (100 mg), boric acid (400 mol%),  $NaCl$  (200 mol%).

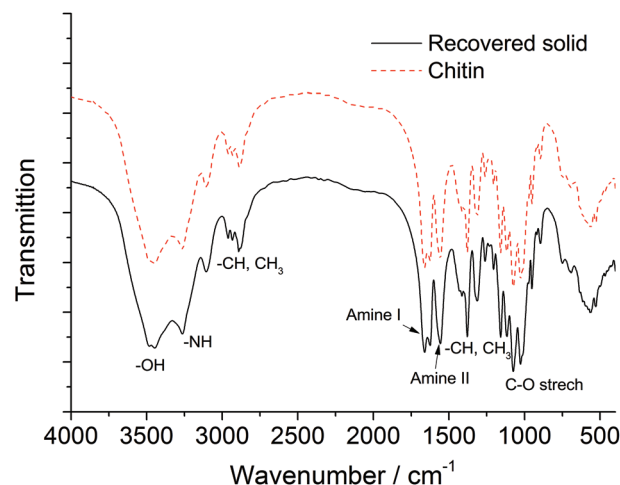


Fig. 4 FTIR spectra of chitin and the recovered solid after the reaction.

speculate that the chitin crystalline region depolymerizes at a slower pace, because the conversion rate slows down significantly compared to the initial conversion. After 2 hours, a maximum 3A5AF yield of 7.5% was achieved with a chitin conversion of 49.7%. As the reaction further progressed, the yield dropped sharply probably due to 3A5AF decomposition. Interestingly, the chitin conversion decreased slightly after 2 hours, which is indicative of the formation of insoluble solids such as char. During the entire reaction, NAG is not observed, suggesting that NAG dehydration is not rate-determining. Since the depolymerization of crystalline chitin is slow and the products are not stable, the 3A5AF yield cannot be further improved simply by prolonging the reaction time.

Chitin and the recovered solids after the reaction (215 °C, 1 h reaction time) have been characterized by FTIR, XRD and EA. As shown in the FTIR spectrum of pure chitin (see Fig. 4, dash line), the bands at 3452 and 3266  $cm^{-1}$  are attributed to the OH and NH stretching, respectively. The shape and intensity of these peaks will change if the hydrogen bonding network in chitin is altered. The bands ranging from 2886 to 2961  $cm^{-1}$  represent CH,  $CH_3$  symmetric stretching and  $CH_2$  asymmetric stretching. And the CH bending, symmetric  $CH_3$  deformation and  $CH_2$  wagging bands appear at 1380 and 1312  $cm^{-1}$ . The peaks at 1629 and 1662  $cm^{-1}$  are assigned to Amide I band (two types of hydrogen bonds in a C=O group with the NH group of the adjacent chain and the OH group of the inter-chain). Amide II band (in-plane N-H bending and C-N stretching mode) and Amide III band (in-plane mode of the CONH group) are observed at 1558 and 1312  $cm^{-1}$ , respectively. The bands ranging from 1027 to 1163  $cm^{-1}$  are attributed to the asymmetric bridge oxygen and C-O stretching.<sup>59,60</sup> In the FTIR spectrum of recovered solid, the shape, position and relative intensity of all characteristic peaks are well preserved, which indicates no appreciable modifications on the chemical structure including functional groups and the hydrogen bonding network.

In the XRD pattern of pure chitin (see Fig. 5), the peak at  $2\theta = 19^\circ$  represents the (110) plane of crystalline chitin,<sup>61</sup> together



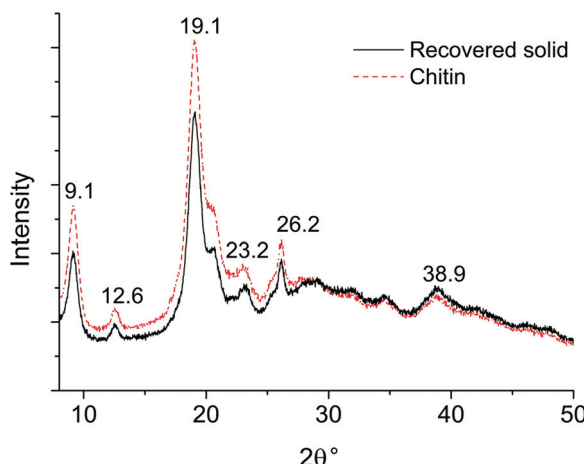


Fig. 5 XRD patterns of chitin and the recovered solid after the reaction.

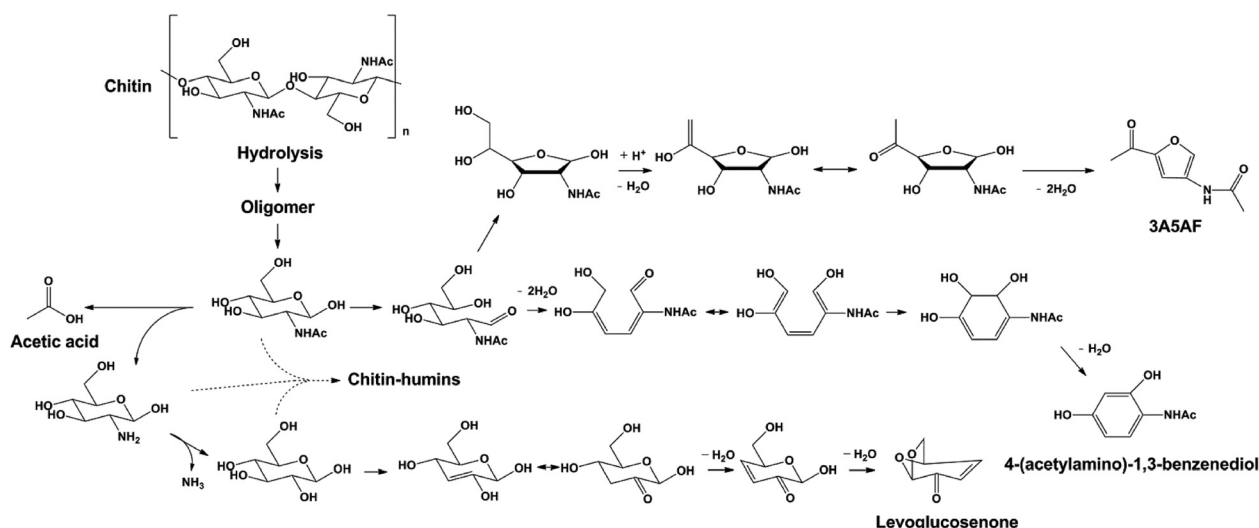
with a few other peaks with much weaker intensity. The XRD pattern of the recovered solid highly resembles that of the chitin standard, suggesting that there is negligible change in the crystalline region. The EA data further corroborate with FTIR and XRD analysis, as the C, H, and N content remains at a similar level in the recovered solid (see Table S1†). According to the EA, the DA of chitin is 99% and the value remains almost unchanged for the recovered solid. From these observations, we can conclude that the unreacted solids maintain the chemical backbone, the hydrogen bonding network, and the crystalline structure of chitin. It is assumed that chitin polymer chains undergo the depolymerization into oligomers and NAG prior to any other transformations towards 3A5AF and side products.

### 3.4. Reaction pathway elucidation

Under optimized conditions, 3A5AF was obtained with *ca.* 7.5% yield despite a much higher chitin conversion (50%).

In the following work, significant effort was spent on the identification of other products generated from chitin, by combining column chromatography, GC-MS, HPLC, EA, GPC, NMR and FTIR analysis. The major product, 3A5AF, was further confirmed by NMR technique after column chromatography separation (see Fig. S6†). From GC-MS a variety of other products have been identified, including levoglucosenone, acetic acid and 4-(acetylamino)-1,3-benzenediol. Besides these, a black solid fraction was obtained after column separation and characterized by GPC, FTIR and EA. It shares some similarities with humins reported in glucose/cellulose conversion,<sup>62</sup> as both are polymeric black solids and have a higher C/H ratio (see Table S1†) than their parent carbohydrates. On the other hand, the structure of the black solid from chitin is not identical with previously reported humin materials. Humin generated from glucose/cellulose conversion are assumed to form by aldol condensation between sugars and furanics, and the furanic and C=C conjugating bands can be observed in FTIR spectra.<sup>63</sup> These bands are absent in the FTIR spectrum of the black solid from chitin. Furthermore, humins from glucose/cellulose contain no nitrogen, whereas the nitrogen content in the black solid (8%) is even higher than that in chitin. We tentatively term this black solid fraction as chitin-humins. GPC analysis indicates that the average molecular weight of chitin-humins is at around 1 kDa (see Fig. S7†). Interestingly, GPC analysis of the raw reaction mixture revealed another fraction of products with  $M_w$  of 3–4 kDa, in addition to small molecules and chitin-humins (see Fig. S8†). This fraction may be the partially depolymerized and solubilized part of chitin generated in the reaction.

Based on these we propose a plausible reaction pathway for the formation of 3A5AF and other products (see Scheme 1). Hydrolysis of chitin is the first step in the reaction, leading to the partially depolymerized chitin, NAG oligomers and eventually NAG. NAG generated *in situ* undergoes three parallel reaction pathways. In the first pathway, 3A5AF is generated via



Scheme 1 Proposed reaction pathway of the formation of other identified products.



a five-membered ring formed from the open ring aldose. The subsequent enolization and dehydration afford the N-containing furan derivative, similar to that proposed in an earlier study.<sup>28</sup> Alternatively, NAG dehydrates to hexatriene, after which keto–enol tautomerism, electrolytic rearrangement and dehydration take place to form a six-membered ring product. The formation of the aromatic compound is not unusual in biomass conversion. For example, 1,2,4-benzenetriol is widely reported in glucose conversion *via* 5-HMF as an intermediate.<sup>64–66</sup>

The difference is that 1,2,4-benzenetriol forms *via* a five-membered furan ring whereas 4-(acetylamino)-1,3-benzenediol more likely forms *via* a six-member ring intermediate. Finally, hydrolysis of acetyl amide in NAG affords acetic acid and amino-sugar. With further deamination and dehydration, levoglucosenone can be generated. The formation pathway of chitin–humin is not fully understood but it should involve condensation reactions between NAG and amino-sugar considering its high nitrogen content.

### 3.5. Mechanism investigation

**3.5.1. Influence of water.** The reaction pathway from chitin to 3A5AF is a combination of hydrolysis and dehydration reactions. Water is required for the hydrolysis step but should have negative effects on the dehydration steps. Furthermore, the solubility of chitin in the solvent is inversely related to water content. The influence of water was examined (see Fig. S9†) by adding 1%, 2%, 4%, 6% and 8% water into the solvent before reaction. The addition of water clearly shows a significant inhibitory effect on chitin conversion to 3A5AF in all cases. For example, both the 3A5AF yield and chitin conversion decrease by *ca.* 50% in the presence of 2% water, whereas the 3A5AF yield drops to 0.5% when 8% water is added. These experiments unambiguously demonstrated the detrimental effect of water. We conclude that the trace amount of water present in chitin and the solvent is sufficient to initiate chitin hydrolysis, and the water produced during subsequent dehydration is sufficient to sustain chitin hydrolysis. The water content should be kept below 1% to enable efficient chitin conversion.

**3.5.2. Poison test.** It is known that boric acid can coordinate with the hydroxyl groups of substrates. During the interaction, complexes with an acyclic structure or five/six-membered-ring chelate structures could be formed.<sup>53</sup> The specific coordination configuration could be differentiated by a simple poison test. If an acyclic complex is formed during the reaction, the conversion will be inhibited by the addition of a simple alcohol such as ethanol. If a five- or six-membered-ring structure is formed, the addition of ethylene glycol (EG) and 1,3-propanediol (1,3-PG) will inhibit the reaction. In the poison tests, ethanol, EG and 1,3-PG (ratio 2 : 1 to the substrate) were added. For chitin conversion (see Fig. 6), ethanol did not affect the product yield. However, upon the addition of EG or 1,3-PG, the 3A5AF yield decreased from *ca.* 4% to 1% and 0.2%, respectively. 1,3-PG seems to be a stronger poison compared with EG. The poison experiments were conducted using

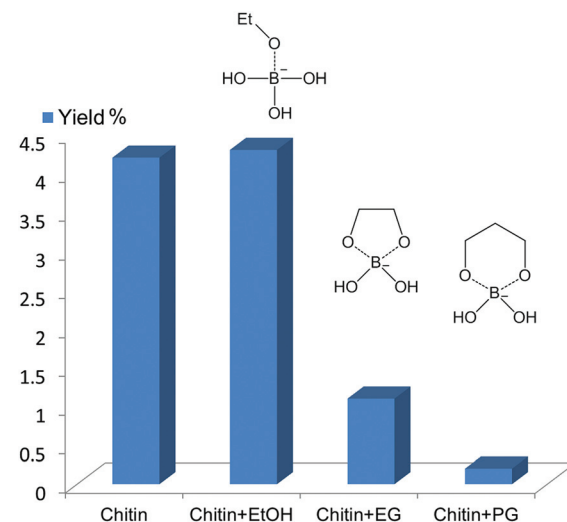
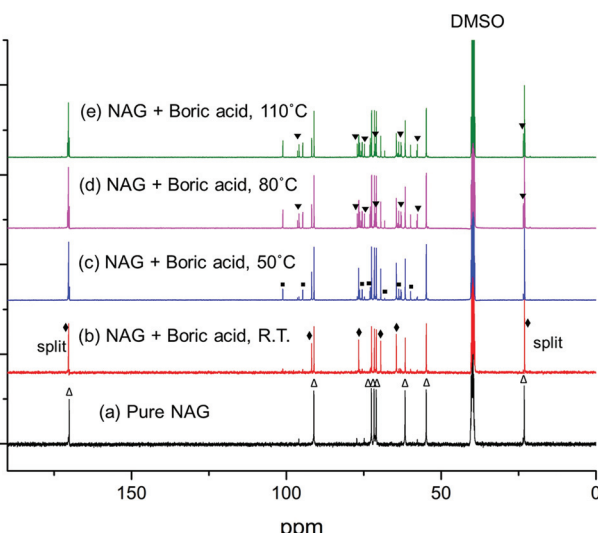


Fig. 6 The inhibition effect of different alcohols as additives. Reaction condition: 215 °C, 1 h, NMP (3 mL), chitin (100 mg), boric acid (200 mol%), NaCl (200 mol%).

NAG as the starting material (see Fig. S10†), and exactly the same trend was observed. Afterward, isopropanol (IPA), 1,2-PG, glycerol (Gly), 1,3-butanediol and 2,3-butanediol were added. IPA had no observable effect on the reaction whereas 1,2-PG, Gly, 1,3- and 2,3-butanediol all inhibited the reaction significantly (data not shown). As such, the 3A5AF formation is achieved *via* five- and six-membered ring boron complexes, and it is likely that the six-membered ring complex is dominant.

**3.5.3. NMR studies.** In order to obtain further understanding on boric acid facilitated chitin transformation into 3A5AF, <sup>1</sup>H, <sup>13</sup>C and <sup>11</sup>B NMR techniques have been utilized. Since the solubility of NAG is much higher than that of chitin and the NMR signal of NAG is much easier to be identified and followed, the measurements were conducted using NAG as a model substrate in the presence of 100 mol% boric acid in DMSO-d<sub>6</sub> (see Fig. 7 for <sup>13</sup>C and Fig. S11† for <sup>1</sup>H NMR). When NAG is freshly dissolved in DMSO-d<sub>6</sub>, the <sup>13</sup>C NMR and <sup>1</sup>H spectra were predominantly by peaks from its  $\alpha$ -anomer. By adding boric acid at room temperature, significant changes were observed in both <sup>1</sup>H and <sup>13</sup>C NMR spectra. Interestingly, two peaks belonging to the proton on OH groups disappear in the <sup>1</sup>H NMR spectrum and several peaks arise (see Fig. S11†). A series of new peaks are also observed in the <sup>13</sup>C NMR spectrum (see Fig. 7b), most of which experience a downfield shift (signal move to larger ppm). It is reported that when saccharides form a complex with boron, a substituent effect of 3–10 ppm to higher frequency can be expected.<sup>67</sup> In accordance with these changes, a new broad peak appears on <sup>11</sup>B NMR compared with pure boric acid (Fig. 8a). <sup>11</sup>B NMR signals alone are not conclusive but by combining <sup>1</sup>H, <sup>13</sup>C, <sup>11</sup>B NMR studies and poison tests, we conclude that each boric acid interacts with two hydroxyl groups and forms a boron containing complex. <sup>1</sup>H NMR of NAG in DMA-d<sub>9</sub> has been investigated previously.<sup>68</sup> By comparison, it appears that the two peaks that





**Fig. 7**  $^{13}\text{C}$  NMR of pure NAG and with boric acid at different temperatures. The sample was maintained at each temperature for 1 hour before NMR analysis.  $\blacktriangledown$  denotes the peaks of  $\beta$ -anomer;  $\blacklozenge$  denotes the peaks assigned to the boron complex;  $\blacksquare$  denotes the peaks assigned to the dimer;  $\triangle$  denotes the peaks for  $\alpha$ -anomer. Note: the peaks at around 23 and 170 ppm are split upon the addition of boric acid, which may not be obviously seen in the figure.

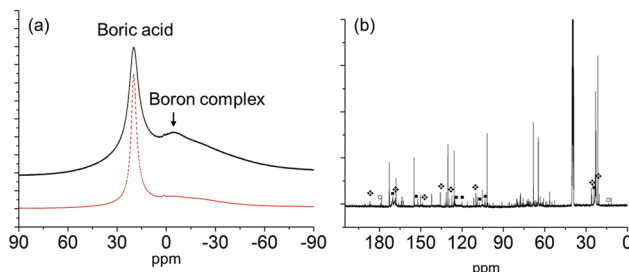


**Fig. 8** (a)  $^{11}\text{B}$  NMR of boric acid (dash line) and boric acid with NAG (solid line) at room temperature; (b)  $^{13}\text{C}$  NMR of the sample in  $\text{DMSO-d}_6$  after heating at  $160\text{ }^\circ\text{C}$  for 1 h.  $\blacklozenge$  denotes the peaks for the major product 3A5AF;  $\blacksquare$  possibly denotes 4-(acetylamino)-1,3-benzenediol;  $\circ$  denotes the peaks for acetic acid.

disappeared in the  $^1\text{H}$  NMR spectrum could be assigned to the hydroxyl groups on  $\text{C}_3/\text{C}_4$  and  $\text{C}_6$ , respectively. The DFT calculation suggests that boron coordinated with OH groups at  $\text{C}_4$  and  $\text{C}_6$  was most stable for glucose conversion in the presence of boric acid.<sup>45</sup> It is not unreasonable to speculate that boric acid interacts with OH groups on  $\text{C}_4$  and  $\text{C}_6$  and forms a six-membered-ring boron complex, in perfect agreement with poison tests.

After heating at 50, 80 and  $110\text{ }^\circ\text{C}$ , the peaks assigned to the boron complex keep decreasing and new peaks intensify concurrently (Fig. 7c–e), indicating that the boron complex is intermediate for further conversion. The new peaks can be categorized into two groups. By referring to the standard  $^{13}\text{C}$  NMR spectra, one group of the rising peaks can be unambiguously assigned to the  $\beta$ -anomer of NAG. Meanwhile, another group is likely to be assigned to the dimer of NAG. The formation of  $\beta$ -anomer

suggests that boric acid facilitates the ring-opening reaction of the  $\alpha$ -anomer, since the linear form of NAG is required for  $\beta$ -anomer formation. At the same time, this provides a plausible explanation for the promotional effect of boric acid, as the formation of 3A5AF starts with the ring opening of NAG. After heating at  $160\text{ }^\circ\text{C}$ , the color of the sample became dark black and a variety of peaks appeared in the  $^{13}\text{C}$  NMR spectrum (see Fig. 8b). The peaks belonging to 3A5AF, 4-(acetylamino)-1,3-benzenediol and acetic acid have been assigned. Levoglucosanone is not found possibly due to its low concentration. There are many other peaks in the carbon–carbon double bond (100–150 ppm) and unsaturated alcoholic alkane range (50–80 ppm), which might be assigned to precursors for chitin–humins and other side products.

## 4. Conclusions

For the first time, direct conversion of chitin into a nitrogen-containing furan derivative (3A5AF) was systematically investigated, opening up a new avenue for generating value-added, renewable chemicals bearing nitrogen. Boric acid is identified as the best additive and NMP as the best solvent. Under optimized conditions, 3A5AF reaches a yield of 7.5% from chitin in two hours. NMR studies and poison tests provided mechanistic insights by confirming the formation of a six-membered ring boron complex intermediate. Water is detrimental to the reaction and its content should be kept below 1%. The entire reaction network from chitin to 3A5AF and side products has been established by a combination of instrumental techniques. Kinetic studies suggest that hydrolysis of the crystalline region of chitin is likely to be rate-determining, and the product is not stable at high temperatures or for elongated reaction times.

The yield of 3A5AF from chitin is low in the current work. Two strategies to further increase the one-pot conversion of chitin into nitrogen containing chemicals such as 3A5AF can be envisaged. Chitin pretreatment may be essential for chitin depolymerization as it can break down the robust structure and hydrogen bonding network effectively. Solvents that exhibit better solubility towards chitin dissolution, such as ionic liquids, could also be attempted. Investigations along these directions are currently underway in the lab.

## Acknowledgements

This work was financially supported by the Start-up Grant from NUS (WBS: R-279-000-368-133) and a MOE Tier-1 project (WBS: R-279-000-387-112).

## Notes and references

- 1 J. R. Rostrup-Nielsen, *Science*, 2005, **308**, 1421–1422.
- 2 C. Somerville, H. Youngs, C. Taylor, S. C. Davis and S. P. Long, *Science*, 2010, **329**, 790–792.



3 G. W. Huber, S. Iborra and A. Corma, *Chem. Rev.*, 2006, **106**, 4044–4098.

4 C. S. K. Lin, R. Luque, J. H. Clark, C. Webb, C. Du, C. S. K. Lin, R. Luque, J. H. Clark, C. Webb and C. Du, *High Energy Dens. Phys.*, 2011, **4**, 1471–1479.

5 A. Fukuoka and P. L. Dhepe, *Angew. Chem., Int. Ed.*, 2006, **118**, 5285–5287.

6 N. Yan, C. Zhao, C. Luo, P. J. Dyson, H. Liu and Y. Kou, *J. Am. Chem. Soc.*, 2006, **128**, 8714–8715.

7 J. B. Binder and R. T. Raines, *J. Am. Chem. Soc.*, 2009, **131**, 1979–1985.

8 N. Yan, Y. Yuan, R. Dykeman, Y. Kou and P. J. Dyson, *Angew. Chem., Int. Ed.*, 2010, **49**, 5549–5553.

9 R.-J. van Putten, J. C. van der Waal, E. de Jong, C. B. Rasrendra, H. J. Heeres and J. G. de Vries, *Chem. Rev.*, 2013, **113**, 1499–1597.

10 N. Yan and P. J. Dyson, *Curr. Opin. Chem. Eng.*, 2013, **2**, 178–183.

11 B. R. Caes, M. J. Palte and R. T. Raines, *Chem. Sci.*, 2013, **4**, 196–199.

12 C. Luo, S. Wang and H. Liu, *Angew. Chem., Int. Ed.*, 2007, **119**, 7780–7783.

13 T. Deng and H. Liu, *Green Chem.*, 2013, **15**, 116–124.

14 H. Kobayashi and A. Fukuoka, *Green Chem.*, 2013, **15**, 1740–1763.

15 F. M. Kerton, Y. Liu, K. W. Omari and K. Hawboldt, *Green Chem.*, 2013, **15**, 860–871.

16 M. Rinaudo, *Prog. Polym. Sci.*, 2006, **31**, 603–632.

17 H. Sashiwa and S.-i. Aiba, *Prog. Polym. Sci.*, 2004, **29**, 887–908.

18 K. Gopalan Nair, A. Dufresne, A. Gandini and M. N. Belgacem, *Biomacromolecules*, 2003, **4**, 1835–1842.

19 H. Sashiwa and Y. Shigemasa, *Carbohydr. Polym.*, 1999, **39**, 127–138.

20 A. K. Metreveli, P. K. Metreveli, I. E. Makarov and A. V. Ponomarev, *High Energy Chem.*, 2013, **47**, 35–40.

21 L. T. Zeng, C. Q. Qin, L. S. Wang and W. Li, *Carbohydr. Polym.*, 2011, **83**, 1553–1557.

22 J. Zawadzki and H. Kaczmarek, *Carbohydr. Polym.*, 2010, **80**, 394–400.

23 A. Einbu and K. M. Varum, *Biomacromolecules*, 2008, **9**, 1870–1875.

24 G. Vaaje-Kolstad, B. Westereng, S. J. Horn, Z. Liu, H. Zhai, M. Sørlie and V. G. H. Eijsink, *Science*, 2010, **330**, 219–222.

25 M. Mascal and E. B. Nikitin, *ChemSusChem*, 2009, **2**, 859–861.

26 K. W. Omari, J. E. Besaw and F. M. Kerton, *Green Chem.*, 2012, **14**, 1480–1487.

27 Y. Wang, C. M. Pedersen, T. Deng, Y. Qiao and X. Hou, *Bioresour. Technol.*, 2013, **143**, 384–390.

28 M. W. Droyer, K. W. Omari, J. N. Murphy and F. M. Kerton, *RSC Adv.*, 2012, **2**, 4642–4644.

29 K. W. Omari, L. Dodot and F. M. Kerton, *ChemSusChem*, 2012, **5**, 1767–1772.

30 X. Hu, Y. Du, Y. Tang, Q. Wang, T. Feng, J. Yang and J. F. Kennedy, *Carbohydr. Polym.*, 2007, **70**, 451–458.

31 Y.-B. Huang and Y. Fu, *Green Chem.*, 2013, **15**, 1095–1111.

32 B. Lindman, G. Karlström and L. Stigsson, *J. Mol. Liq.*, 2010, **156**, 76–81.

33 C. K. S. Pillai, W. Paul and C. P. Sharma, *Prog. Polym. Sci.*, 2009, **34**, 641–678.

34 H. Kobayashi, Y. Ito, T. Komanoya, Y. Hosaka, P. L. Dhepe, K. Kasai, K. Hara and A. Fukuoka, *Green Chem.*, 2011, **13**, 326–333.

35 J. Fan, M. De Bruyn, V. L. Budarin, M. J. Gronnow, S. Breeden, D. J. Macquarrie, J. H. Clark, P. S. Shuttleworth, J. Fan, M. De Bruyn, V. L. Budarin, M. J. Gronnow, S. Breeden, D. J. Macquarrie, J. H. Clark and P. S. Shuttleworth, *J. Am. Chem. Soc.*, 2013, **135**, 12728–12731.

36 O. A. El Seoud, H. Nawaz and E. P. Aréas, *Molecules*, 2013, **18**, 1270–1313.

37 J. N. Chheda, Y. Roman-Leshkov and J. A. Dumesic, *Green Chem.*, 2007, **9**, 342–350.

38 M. Ohara, A. Takagaki, S. Nishimura and K. Ebitani, *Appl. Catal., A*, 2010, **383**, 149–155.

39 J. Wang, J. Ren, X. Liu, G. Lu and Y. Wang, *AIChE J.*, 2013, **59**, 2558–2566.

40 J. N. Chheda and J. A. Dumesic, *Catal. Today*, 2007, **123**, 59–70.

41 A. S. Amarasekara, L. D. Williams and C. C. Ebede, *Carbohydr. Res.*, 2008, **343**, 3021–3024.

42 Y. Román-Leshkov, J. N. Chheda and J. A. Dumesic, *Science*, 2006, **312**, 1933–1937.

43 B. F. M. Kuster and H. S. van der Baan, *Carbohydr. Res.*, 1977, **54**, 165–176.

44 T. S. Hansen, J. M. Woodley and A. Riisager, *Carbohydr. Res.*, 2009, **344**, 2568–2572.

45 T. Ståhlberg, S. Rodriguez-Rodriguez, P. Fristrup and A. Riisager, *Chem.-Eur. J.*, 2011, **17**, 1456–1464.

46 E. A. Khokhlova, V. V. Kachala and V. P. Ananikov, *ChemSusChem*, 2012, **5**, 783–789.

47 T. S. Hansen, J. Mielby and A. Riisager, *Green Chem.*, 2011, **13**, 109–114.

48 S. Zhao, M. Cheng, J. Li, J. Tian and X. Wang, *Chem. Commun.*, 2011, **47**, 2176–2178.

49 Z. Sun, M. Cheng, H. Li, T. Shi, M. Yuan, X. Wang and Z. Jiang, *RSC Adv.*, 2012, **2**, 9058–9065.

50 Y. Zhang, V. Degirmenci, C. Li and E. J. M. Hensen, *ChemSusChem*, 2011, **4**, 59–64.

51 E. A. Pidko, V. Degirmenci and E. J. M. Hensen, *ChemCatChem*, 2012, **4**, 1263–1271.

52 H. Zhao, J. E. Holladay, H. Brown and Z. C. Zhang, *Science*, 2007, **316**, 1597–1600.

53 S. Hu, Z. Zhang, J. Song, Y. Zhou and B. Han, *Green Chem.*, 2009, **11**, 1746–1749.

54 Z. Zhang, Q. Wang, H. Xie, W. Liu and Z. Zhao, *ChemSusChem*, 2011, **4**, 131–138.

55 Y. Su, H. M. Brown, X. Huang, X.-d. Zhou, J. E. Amonette and Z. C. Zhang, *Appl. Catal., A*, 2009, **361**, 117–122.

56 J. Potvin, E. Sorlien, J. Hegner, B. DeBoef and B. L. Lucht, *Tetrahedron Lett.*, 2011, **52**, 5891–5893.



57 R. C. Remsing, R. P. Swatloski, R. D. Rogers and G. Moyna, *Chem. Commun.*, 2006, 1271–1273.

58 Y. Wang, Y. Chang, L. Yu, C. Zhang, X. Xu, Y. Xue, Z. Li and C. Xue, *Carbohydr. Polym.*, 2013, **92**, 90–97.

59 M. Osada, C. Miura, Y. S. Nakagawa, M. Kaihara, M. Nikaido and K. Totani, *Carbohydr. Polym.*, 2013, **92**, 1573–1578.

60 F. G. Pearson, R. H. Marchessault and C. Y. Liang, *J. Polym. Sci.*, 1960, **43**, 101–116.

61 G. Cárdenas, G. Cabrera, E. Taboada and S. P. Miranda, *J. Appl. Polym. Sci.*, 2004, **93**, 1876–1885.

62 S. K. R. Patil and C. R. F. Lund, *Energy Fuels*, 2011, **25**, 4745–4755.

63 I. van Zandvoort, Y. Wang, C. B. Rasrendra, E. R. H. van Eck, P. C. A. Bruijnincx, H. J. Heeres and B. M. Weckhuysen, *ChemSusChem*, 2013, **6**, 1745–1758.

64 Z. Srokol, A.-G. Bouche, A. van Estrik, R. C. J. Strik, T. Maschmeyer and J. A. Peters, *Carbohydr. Res.*, 2004, **339**, 1717–1726.

65 A. Kruse and A. Gawlik, *Ind. Eng. Chem. Res.*, 2002, **42**, 267–279.

66 T. M. Aida, Y. Sato, M. Watanabe, K. Tajima, T. Nonaka, H. Hattori and K. Arai, *J. Supercrit. Fluids*, 2007, **40**, 381–388.

67 R. van den Berg, J. A. Peters and H. van Bekkum, *Carbohydr. Res.*, 1994, **253**, 1–12.

68 M. Vincendon, *Die Makromol. Chem.*, 1985, **186**, 1787–1795.

